Quantifying footprint

Gary F. Margrave, Devon Canada Corporation

SUMMARY

A method is presented to numerically estimate the degree of seismic acquisition footprint in a 3D seismic volume. Operating on time (or depth) slices, the method first constructs digital representations of the source and receiver grids and then these grids are crosscorrrelated with a chosen time slice. For orthogonal source and receiver grids, the procedure is especially simple since only correlation lags orthogonal to the source or receiver lines need be examined. Footprint causes a periodicity in the crosscorrelations whose period is the ratio between the line spacing and the image bin dimension. In a series of examples using real data, it is observed that the grid correlation measurement is much more sensitive than mere visual assessment to detect footprint. This is especially useful for comparing the effectiveness of alternative methods of footprint suppression.

INTRODUCTION

In seismic exploration, the geometry, or positions, of sources and receivers is a very important decision that has impact on everything from the cost of acquisition, through data processing, and to the final image. Rarely is it possible or economically feasible to use an optimally dense grid for either sources or receivers and compromises must be accepted. These practical realities have impact on the quality of the final seismic image in numerous ways including (1) imperfect noise suppression, (2) limited resolution, (3) spatial aliasing of signal and noise, (4) imprint of the acquisition grid on the image. While all of these are important, it is the last one that is the topic of this paper and such an imprint will be called *footprint*. In a 3D land survey, common practice is to lay out the sources and receivers in similar grids that are orthogonal to one another (Figure 1). Taken together, these grids sample both x and y directions densely but each grid also samples one of the principal directions very coarsely. This coarse sampling inevitably leads to artefacts in the final image which often echo the geometry of the acquisition grids. Such artefacts are commonly called footprint.

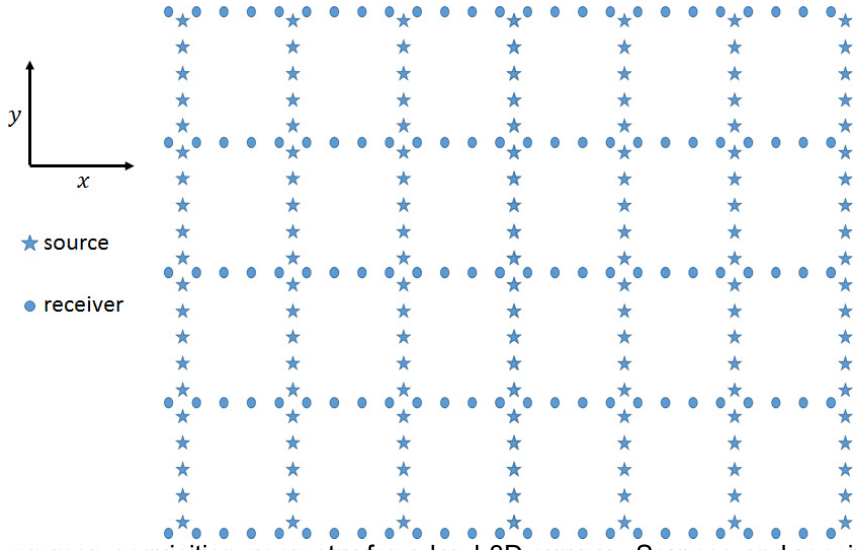

Figure 1. A common acquisition geometry for a land 3D survey. Sources and receivers are laid out in identical, but orthogonal grids. Each grid consists of densely sampled lines with large separation between lines. Dense sampling in one grid occurs in the orthogonal direction to dense sampling in the other grid.

A number of methods have been proposed for reducing, or suppressing, footprint. Among these are (1) Reducing the acquisition line spacing (e.g. Hong-jun et al, 2011), (2) Wavenumber filtering of time slices (e.g. Soubaras 2002, Falconer and Marfurt, 2008), (3) Truncated SVD filtering (Al-Bannagi et al. 2005), (4) Geostatistical filtering (Hober et al., 2003) and undoubtedly many more. However, this paper is not about presenting a new technique for footprint suppression, but rather to suggest a simple and objective method to quantify the level of footprint in a dataset and to objectively evaluate the degree of suppression achieved by a given method. Essentially the proposed quantification involves constructing digital representations of the acquisition grids and measuring the crosscorrelation between these digital grids and time slices from a seismic survey. This method is available via software in the CREWES Matlab release: seisplotsvd_foot.m and seisplotsvd_sep.m .

METHOD

I will present the method and some basic results by way on an illustrative example using a 3D survey conducted by Devon Energy. Shown in Figure 2 is a time slice from this survey which exhibits west-east streaking that was judged to be footprint. In this case, the receiver lines are oriented west-east while the source lines are north-south. So, is this truly receiver-line footprint and is there any source-line footprint? The image shown is migrated data with a bin size of 82.5x82.5 ft. The spacing between receiver lines was 10 times the bin size or 825 ft. and the source lines were similarly spaced. The time slice in question can be regarded as a matrix having 747 rows (the number of inlines) and 550 columns (the number of crosslines) where there is one matrix sample for each 82.5 ft^2 bin in the image. The construction of digital representations of the receiver grid therefore involves constructing a similar sized matrix which is zero everywhere except at receiver locations where it takes the value 1. The source grid is similarly constructed. Rather than make these grids perfectly sharp 1/0 constructions, I then applied a gentle isotropic wavenumber

filter that slightly fuzzes the amplitude transition. Figure 3 shows the source and receiver synthetic grids constructed for this purpose.

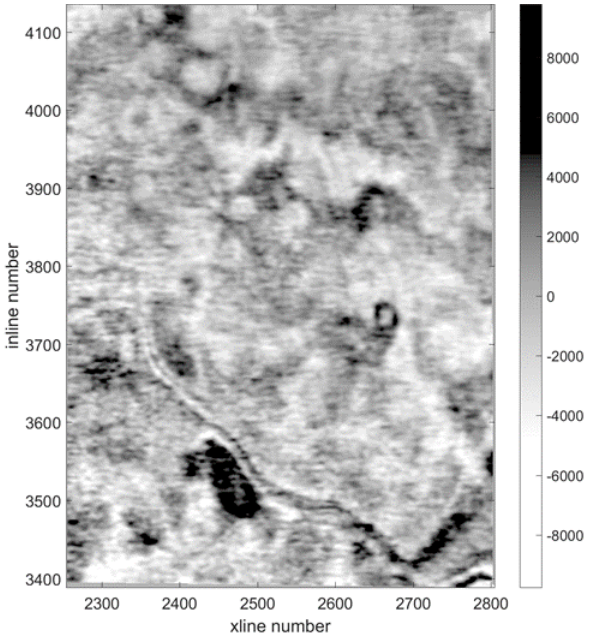

Figure 2: A time slice from the example survey showing obvious east-west (right-left) streaking. The receiver lines were oriented east-west and the source lines north-south.

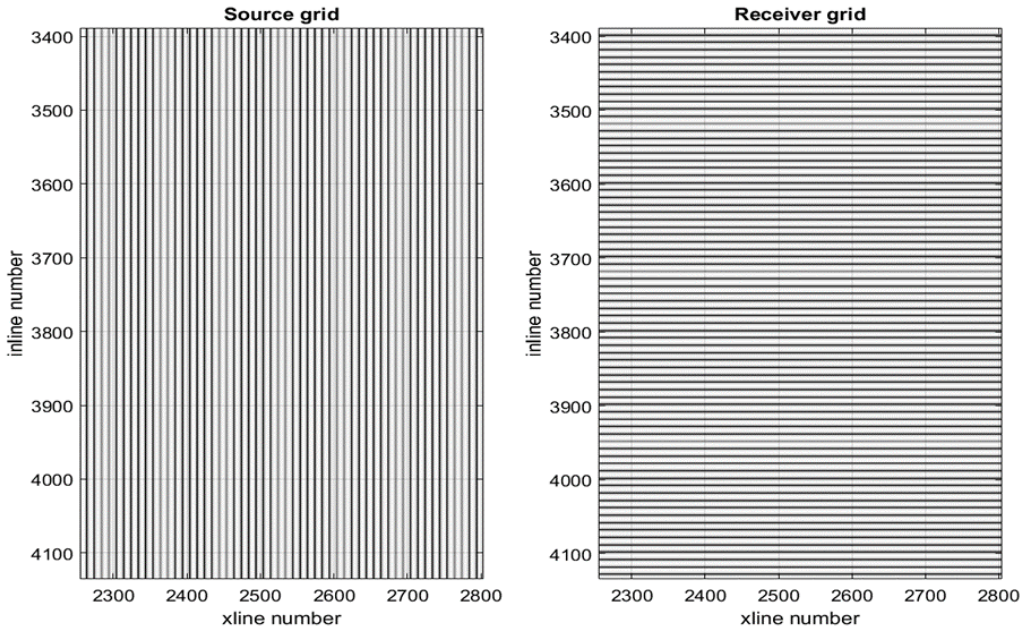

Figure 3. Source and receiver idealized acquisition grids are shown. The spacing between source lines is 825 ft. which is the same as the receiver-line spacing. The apparent slight periodic amplitude variation is a graphical illusion (see Figure 4).

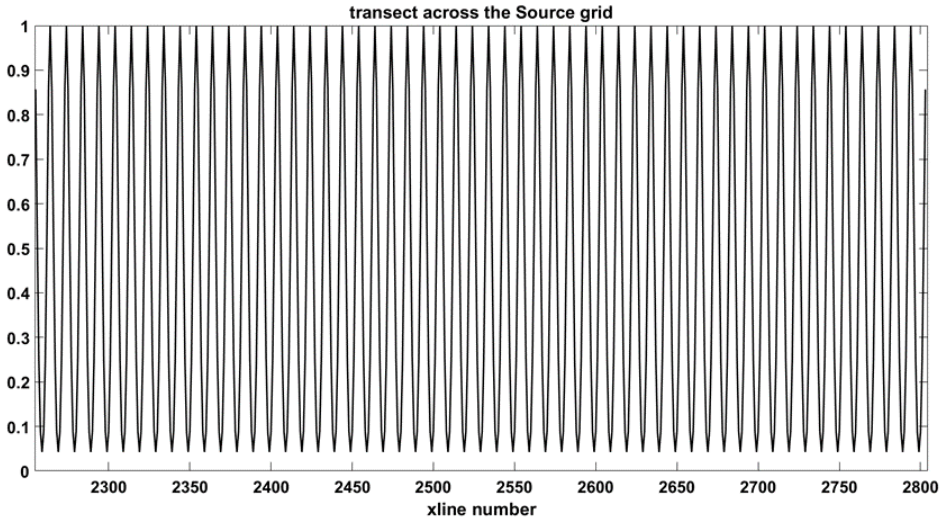

Figure 4. A transect across the source grid in Figure 3 illustrating its basic "comb" nature. The grids were first constructed as idealized 1/0 matrices but a gentle isotropic wavenumber filter has been applies to slightly soften the transition. A transect across the receiver grid is similar and not shown.

In the construction of these grids, the exact locations of source and receiver are not important and not used. What is used is the spacing between source and receiver lines which was carefully constructed to be 825 ft. These represent nominal grids and no attempt has been made to honor departures from ideal grids that occurred during actual acquisition due to cultural obstacles and the like.

The method proposed here is to crosscorrelate the source and receiver grids with the time slice. Given the symmetry of the source grid, only correlation lags in the xline direction need to be calculated and, similarly, only inline lags are required for the receiver grid. Furthermore, these grids have a periodicity of 10 in the direction orthogonal to their symmetry and so it is sufficient to examine lags from -10 to +10 in each case. At this point, it helps to recall that a 2D crosscorrelation is just an alignment of the image with the grid shifted by some lag and then a pointwise multiplication of the samples that align followed by a sum of all such products. This is then repeated for all desired lags and normalized so that a perfect correlation gives a value of 1.0. It should now be evident by the precise source/receiver locations are not required. At some lag, k, the source grid will align with the actual grid and then will align again with ± 10 lags from the lag k. What we are looking for is a periodicity of 10 in these computed correlations as an indication of footprint.

I have found it most revealing to crosscorrelate the grids with the absolute value of the time slice rather than the slice itself. Assume for arguments sake that the footprint is imposed on the time slice as a multiplication of the grid and the slice. The slice will have both positive and negative values and the multiplication by the grid will make the positives more positive and the negatives more negative. In the crosscorrelation, the values that align with the grid are selected and summed and thus the positives and negatives will tend to cancel. Using the absolute value of the time slice avoids this effect. Numerical experimentation with this real dataset has confirmed a much stronger foot[print signal is seen with the absolute value technique.

Figure 5 shows the result of the grid correlations with respect to the time-slice shown in Figure 2. There is a clear periodicity of 10 in both correlation functions indicating the presence of both receiver and source footprint. The receiver-line footprint was visually anticipated from inspection of Figure 2 but the source-line footprint was not (at least to my eye). This is a first indication of the value of objective measures. They may well detect more than does the eye.

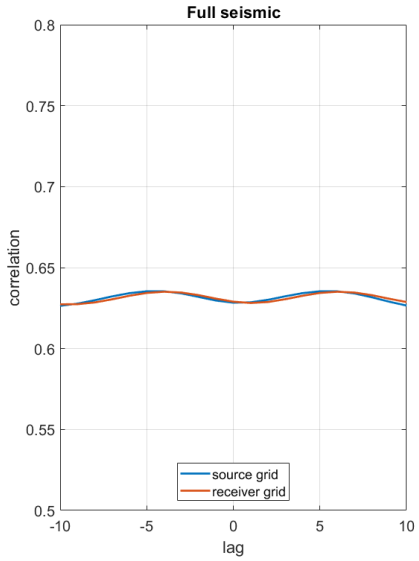

Figure 5. The result of the grid correlations described in the text. The acquisition grids shown in Figure 3 were crosscorrelated in 2D with the image shown in Figure 2. For the source grid, the lags are in the west-eat direction while for the receiver grid they are in the north-south direction.

TESTS ON FOOTPRINT SUPPRESSION ALGORITHMS

This section is an extended discussion of the use of grid correlations to evaluate the performance of two different footprint suppression algorithms. One algorithm is original here and will be described fully while the other is a vendor proprietary method whose details are sequestered.

Footprint suppression by SVD separation and wavenumber filtering

The method of Al-Bannagi et al. (2005) used SVD (singular-value decomposition) to suppress footprint by essentially choosing to discard those singular values that fall beneath a threshold (i.e. threshold filtering). (They applied SVD not to the time slice itself but to a reorganized version called a Hankel matrix.) This is an appealing idea but why should the footprint be confined to small singular values? For those new to SVD, it is a matrix decomposition of the form $A = USV^T$ where all normal-sized symbols are matrices, A represents the seismic time slice, U and V^T are data-dependent "rotation matrices" which are usually uninteresting, while S is a diagonal matrix with the singular values arrayed along the diagonal. Think of the singular values as the "genes" of the seismic matrix and the rotation matrices being the instructions for assembling the genetic information. The singular values are ordered from largest to smallest and the number of them is the smaller of the row or column dimensions of A (550 in this case). Figure 6 shows a separation of the time slice of Figure 2 into a *gross* part, A_g, and a *detail*, A_d, using SVD. This separation

requires the choice of a cutoff singular value, s_c, and then $A_g = US_cV^T$ and $A_d = A - A_g$. Here S_c is derived from S by setting all singular values smaller than s_c to zero. The singular values themselves are plotted at far right (blue curve) and s_c has been chosen as the 10^{th} largest singular value. Visual inspection suggests that there is more footprint in A_g than A_d; however we will soon see that is not so. Figure 7 is a similar separation but uses a smooth rather than a sharp cutoff. These figures were created by the Matlab function *seisplotsvd_sep* which allows interactive adjustment of the cutoff.

Given such a separation, we can now apply wavenumber filtering to each part using potentially different filter parameters. A very simple wavenumber filter is employed here. The time slice is transformed into the 2D wavenumber domain, multiplied by a 2D Gaussian, and then inverse transformed. The only parameter choice is the standard deviation of the Gaussian which is expressed as a fraction of the wavenumber Nyquist. The narrower the Gaussian, the stronger is the suppression of the higher wavenumbers. So a value of 1 is essentially no filtering while 0.125 means that the Gaussian standard deviation is 1/8 of the Nyquist or largest wavenumber.

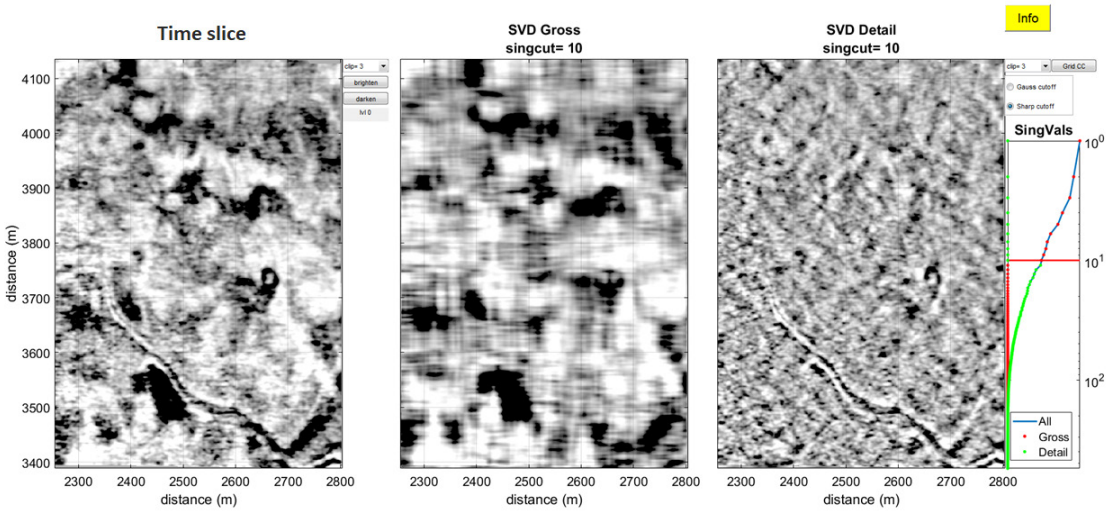

Figure 6. The time slice of Figure 2 is shown separated into gross and detail as determined by a cutoff singular value of number 10. The singular values are plotted at far right (blue curve) using a logarithmic axis.

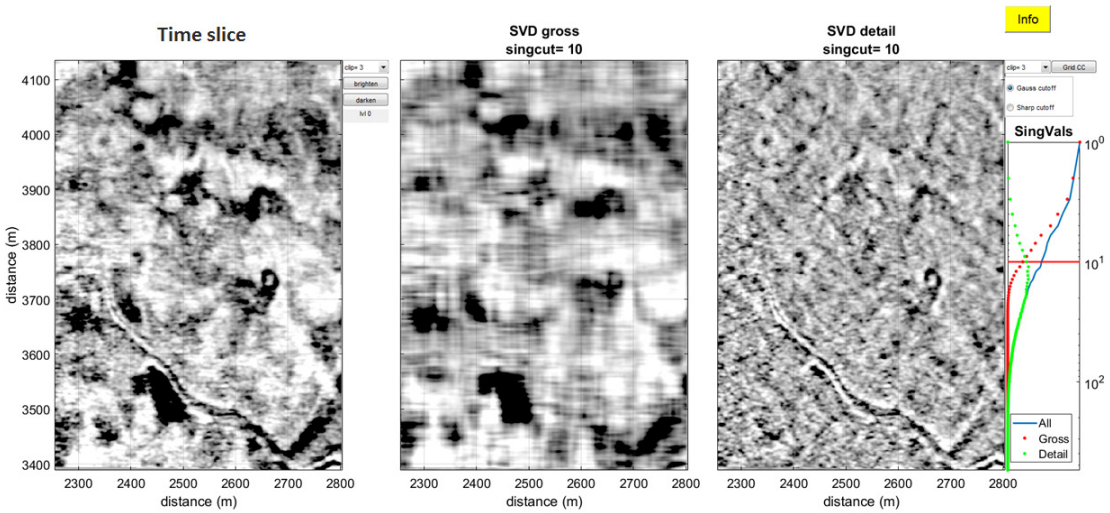

Figure 7. Similar to Figure 10 except that the singular value cutoff is not sharp but rather formed with a Gaussian taper.

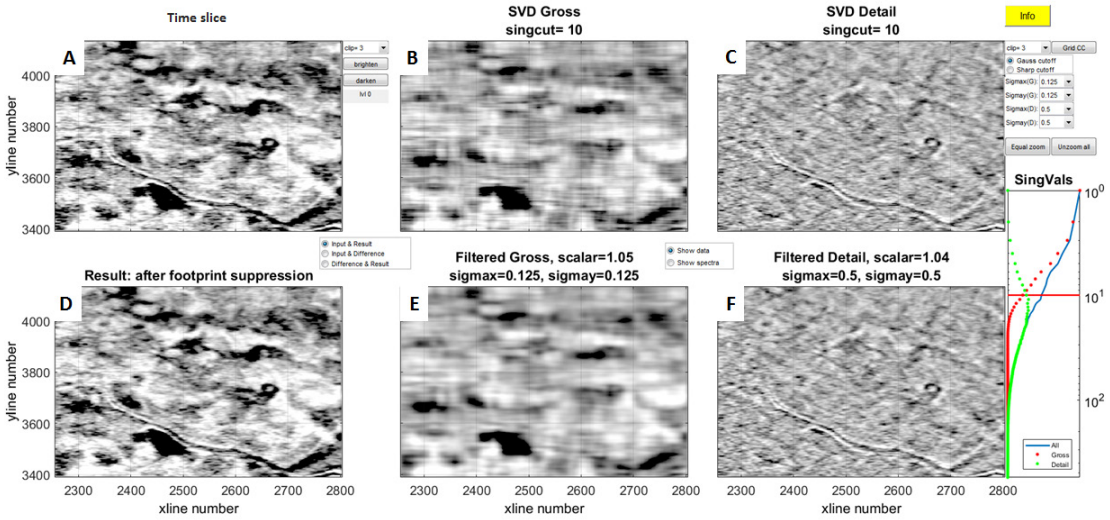

Figure 8. Illustrating the results of a particular wavenumber filter on the SVD separation of Figure 7. A, B, and C are the panels in Figure 7 before wavenumber filtering while D, E, and F are after. In this case, the gross part was filtered with standard deviation $\sigma = 0.125$ which is moderately severe. The detail part was lightly filtered with $\sigma = 0.5$.

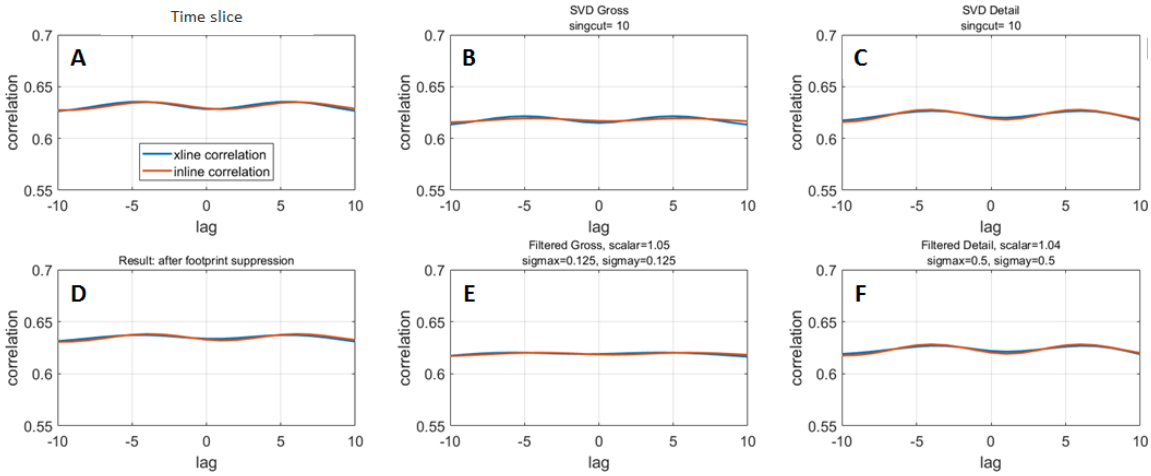

Figure 9. Grid correlations for the six panels of Figure 8. It is apparent that there is strong footprint in both gross and detail and the wavenumber filtering has suppressed it in the gross part.

A first example of wavenumber filtering after SVD separation is shown in Figure 8. The three top panels show the separation of Figure 7 and the three bottom panels show their response to the wavenumber filters. In this case the gross part was filtered more harshly with a standard deviation of $\sigma = 1/8$ Nyquist while the detail was treated lightly with $\sigma = 1/2$. Visual inspection might suggest this has been a moderately successful suppression of footprint. For a more objective assessment, Figure 9 shows the grid correlations for the six panels of Figure 8. A first observation is that both gross and detail show strong footprint and the wavenumber filtering has only suppressed the footprint in gross. Figures 10 and 11 show a second result of wavenumber filtering where both gross and detail were subjected to the same $\sigma = 1/8$ filter. (In this case the SVD separation was unnecessary but is shown for ease of comparison.) It is apparent that the second wavenumber filter has more completely suppressed the footprint but at the expense of greater spatial smearing.

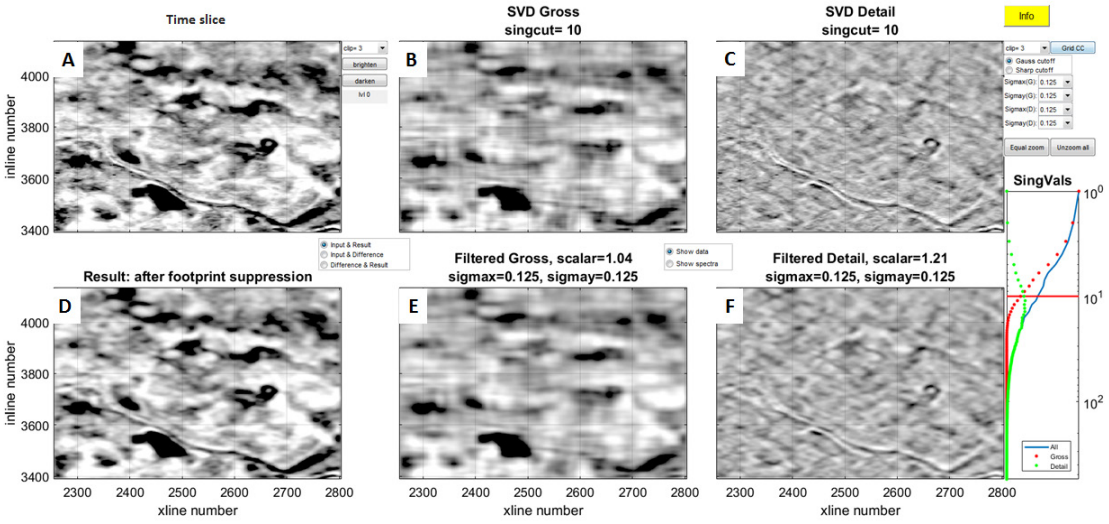

Figure 10. Similar to Figure 8 except that both gross and detail were strongly filtered with a $\sigma = 0.125$ wavenumber filter. The grid correlations are shown in the next figure.

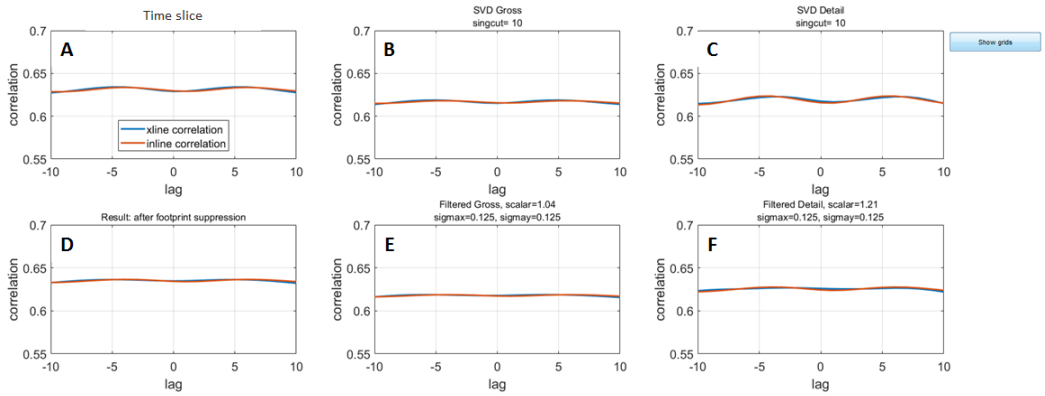

Figure 11. Grid correlations for each panel of Figure 10. In comparison to the result in Figures 8 and 9, there has been stronger suppression of footprint in this case.

A second example is shown in Figure 12. In this case the result in panel A is after footprint suppression by a vendor-supplied geostatistical process, and panels B and C show an SVD separation on this result. Panels D, E, and F show a subsequent gentle wavenumber filter applied to the vendor result. The grid correlations for these six panels are shown in Figure 13. From these it can be inferred that the vendor has reduced the footprint somewhat in the gross portion but less so in the detail. In the subsequent wavenumber filtering, further footprint suppression was achieved but at the expense of some loss of detail.

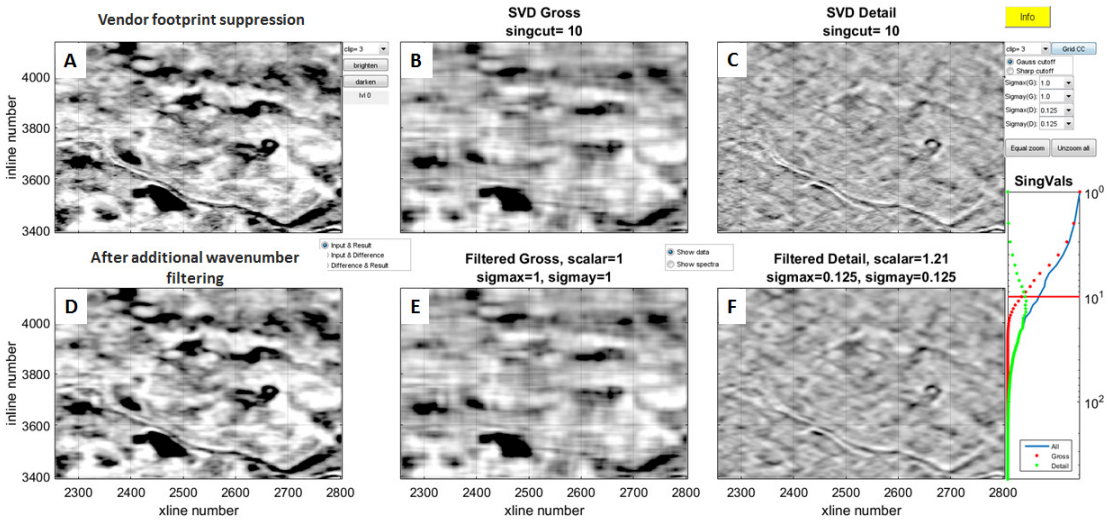

Figure 12. Here is an analysis of footprint suppression done on the time slice of Figure 2 by a vendor-supplied geostatistical filtering technique. Panel A shows the vendor result while panels B and C are its separation into gross and detail. Panels D, E, and F show the application of a further wavenumber filter to the vendor result. The next figure shows the grid correlations.

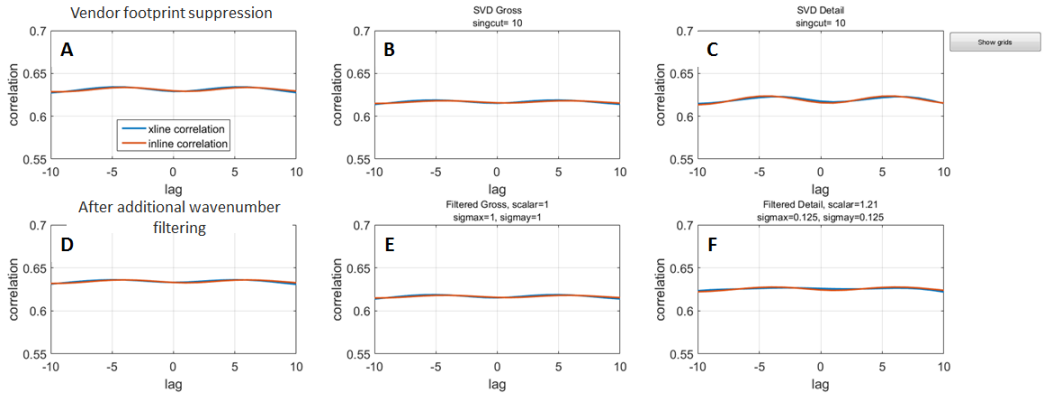

Figure 13. Here are grid correlations of the six panels of Figure 12. It is apparent that the geostatistical method has done some suppression on the gross part but very little on the detail. The application of the further wavenumber filter was required to get similar results to Figure 11.

There are essentially four different results from footprint suppression shown in this paper. These are: (1) moderate wavenumber filtering (Figure 8), (2) harsh wavenumber filter (Figure 10), (3) Vendor geostatistical processing (Figure 12, panel A), and (4) Vendor result with additional gentle wavenumber filtering (Figure 12, panel D). These results are summarized in Figures 14 and 15. From the grid correlations, results (1) and (3) have similar moderate levels of footprint reductions while results (2) and (4) also show similar, but stronger levels. Despite these similarities, the visual appearances of the results are quite different. For further understanding, I turn now to difference plots.

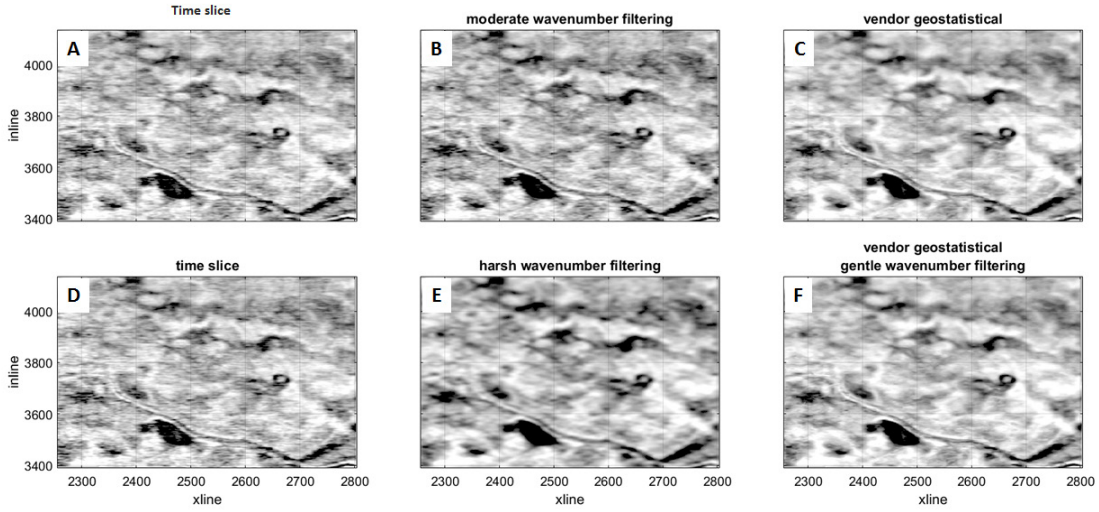

Figure 14. This is a group comparison of all of the results discussed in this paper. Panels A and D are identical with both showing the input time slice of Figure 2. Panels B and E show the moderate and harsh wavenumber filtering results of Figures 8 and 10. Panels C and F show the vendor geostatistical result and a subsequent wavenumber filter from Figure 12. The grid correlations are found in Figure 15.

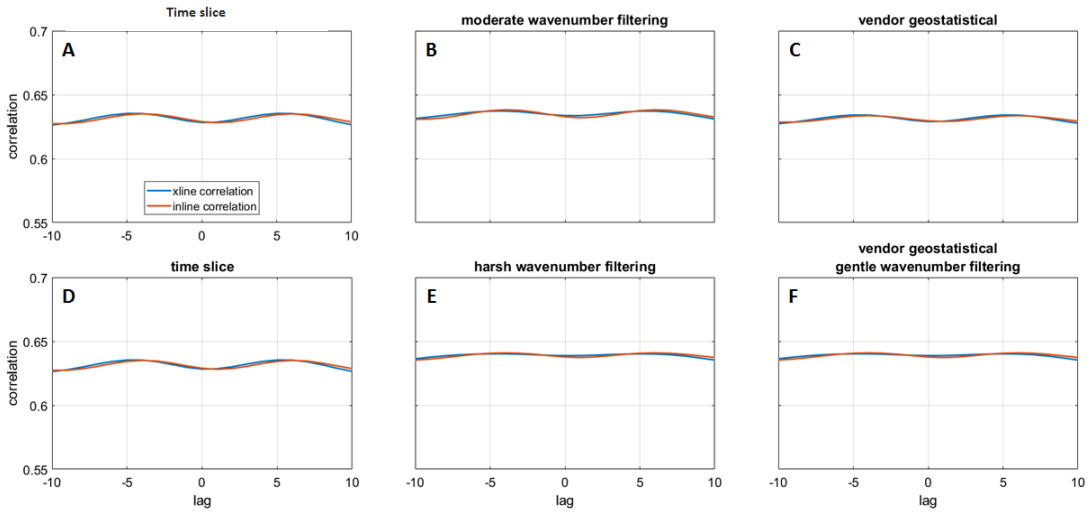

Figure 15. Grid correlations for the panels of Figure 14.

Figures 16-19 show differences between the four wavenumber suppression results and the original time slice. Then Figures 20 and 21 show differences between the two sets of suppression results that achieved similar suppression levels. Examining Figure 16 showing the moderate wavenumber filtering, it is apparent that the difference contains only linear artefacts that parallel the acquisition grids. So we can be confident that the geology was not altered; however, from the grid correlations we can also be sure that significant footprint remains. The harsher wavenumber filter that did suppress the footprint, has also removed some geology (Figure 17). On the other hand, the vendor result, which had similar footprint suppression to the moderate wavenumber filter, shows a mostly random difference but some slight evidence of geology (Figure 18). When this result was passed through a gentle wavenumber filter, suppression similar to the harsh wavenumber filter was achieved but at the expense of more geological leakage.

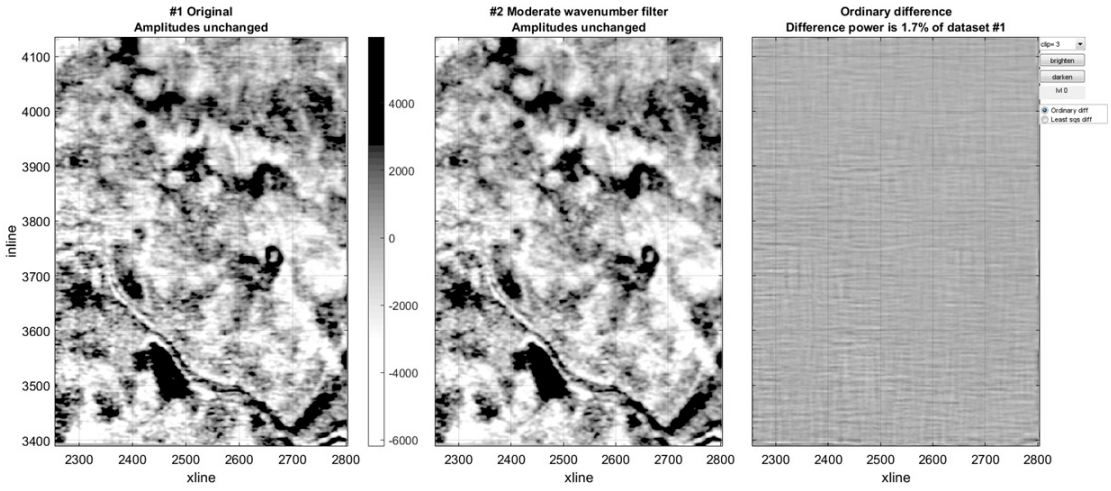

Figure 16. Illustrating the difference between moderate wavenumber filtering and the original time slice. The difference plot shows mostly linear east-west and north-south artefacts which can plausibly be footprint. The difference power is 1.7% of the original.

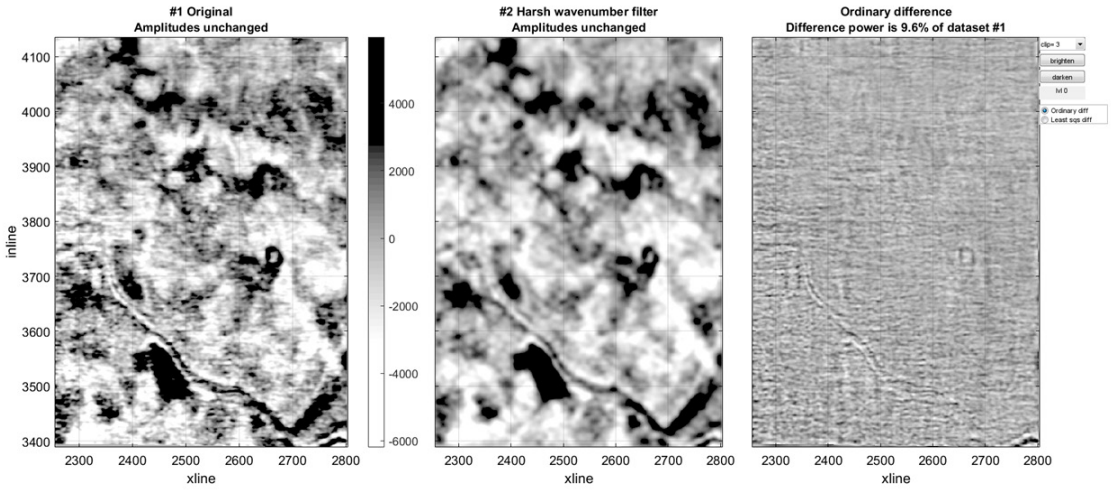

Figure 17. The difference between the harsh wavenumber filter and the original. The difference now shows some geology and the difference power is 9.6% of the original.

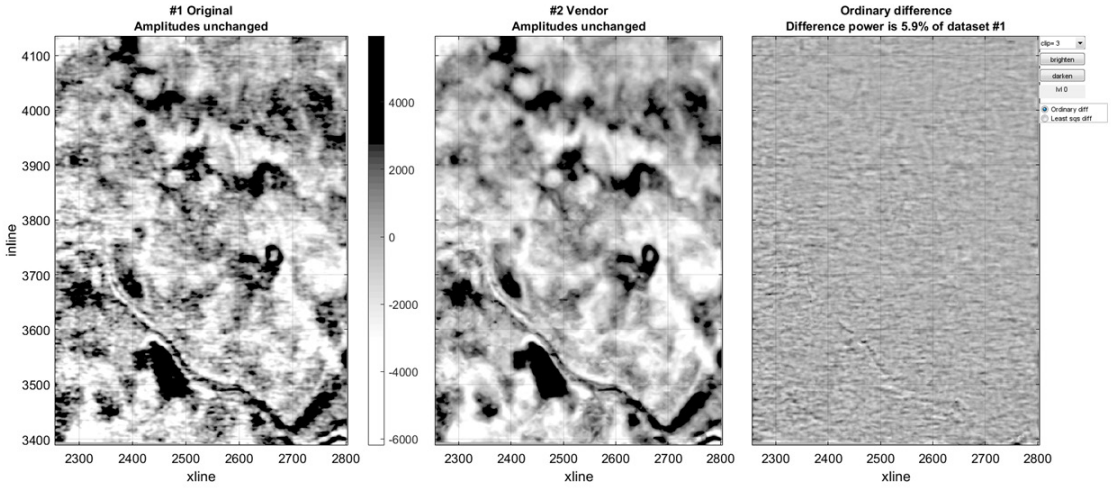

Figure 18. The difference between the Vendor geostatistical solution and the original. There is some geology in the difference and the difference power is 5.9% of the original.

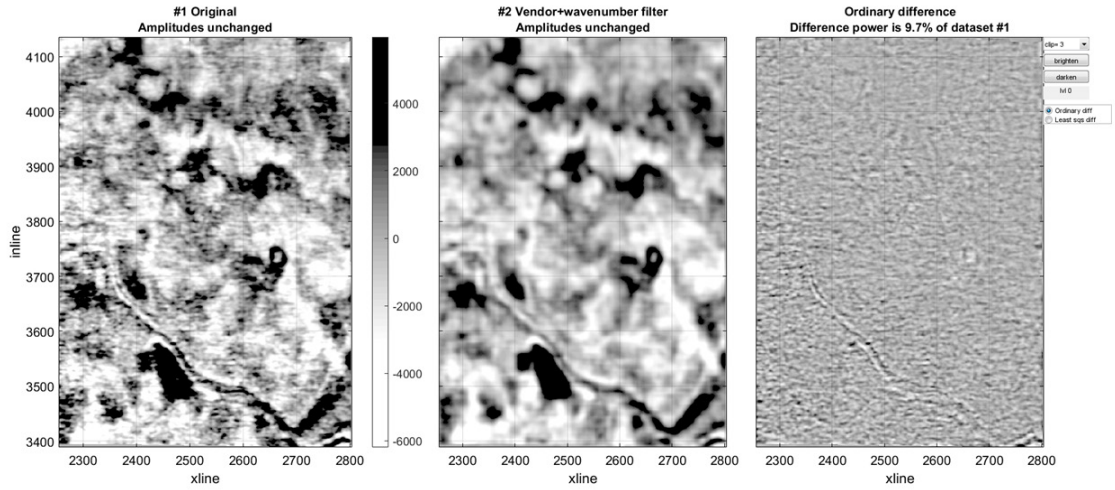

Figure 19. The difference between the Vendor solution with additional wavenumber filtering and the original. There is considerable geology in the difference and the difference power is 9.7% of the original.

The final two comparisons are (Figure 20) between the moderate wavenumber filter and the vendor result and (Figure 21) between the harsh wavenumber filter and the vendor result with a subsequent gentle wavenumber filter. These comparisons are relevant because they are between results with similar suppression levels but with very different techniques. In Figure 20, it is apparent that the vendor result did a much better job suppressing "random noise" and produced a smoother result. It is also apparent, as we saw before, that the vendor result touched the geology a bit more strongly. In the final comparison, it seems that there are detail differences everywhere but it is difficult to choose a preference.

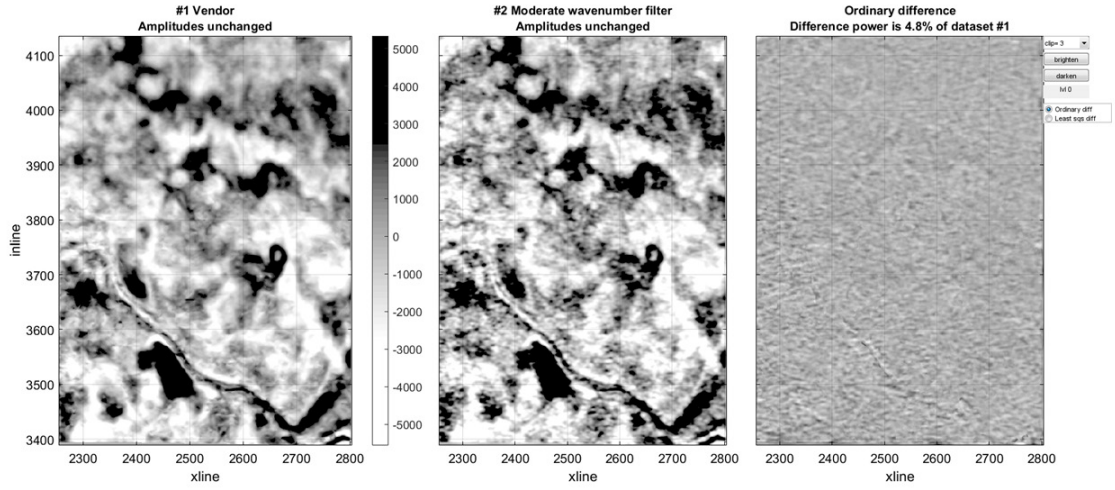

Figure 20. The difference between the Vendor solution and the moderate wavenumber filter. These solutions achieved similar levels of footprint suppression but are quite distinct in their detail.

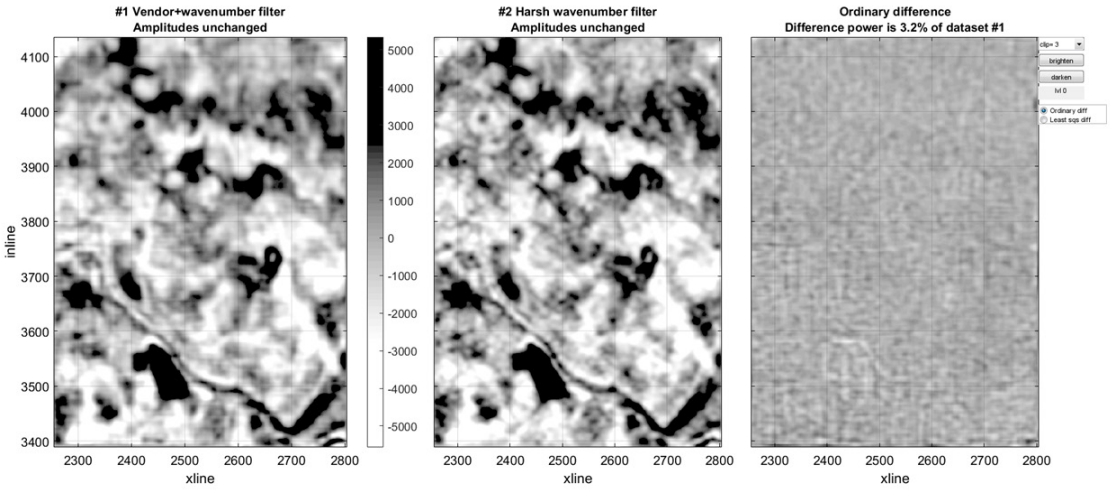

Figure 21. The difference between the Vendor solution with additional wavenumber filtering and the harsh wavenumber filter. These solution achieved similar levels of footprint suppression but are quite dissimilar in detail.

SUMMARY AND CONCLUSIONS

As was mentioned in the introduction, this paper did not intend to introduce a better method of footprint suppression but rather to suggest an objective method of assessing the quality of the suppression. This method uses 2D crosscorrelations between the seismic time slices and numerical representations of the source and receiver acquisition grids. Footprint is indicated by the observation of a periodicity in these crosscorrelations. This technique then gives an objective measure that can complement the more common visual assessment and difference plotting. An extensive example was given in which four different suppression results were compared, not to choose the best one, but rather to illustrate the value of grid correlations in the assessment. In the end, the methods examined were unable to achieve strong footprint suppression without some alteration of the geology.

ACKNOWLEDGEMENTS

I thank the sponsors of CREWES, especially Devon Energy, for their support. My thanks to my colleagues at Devon for their insight and suggestions.

REFERENCES

Al-Bannagi, M., K. Fang, P. G. Kelamis, and G. S. Douglass, 2005, Acquisition footprint suppression via the truncated SVD technique: Case studies from Saudi Arabia: The Leading Edge, 24, 832–834.

Falconer, S., and K. J. Marfurt, 2008, Attribute-driven footprint suppression, 78th Annual International Meeting, SEG, Expanded Abstracts.

Hober, H., T. Coleou, D. Le Meur, E. Angerer, P. Lanfranchi, and D. Lecerf, 2003, On the use of geostatistical filtering techniques in seismic processing, SEG international Exposition and Annual Meeting, Expanded Abstracts.

Hong-jun, Z., W. Lin, and W. Jun, 2011, Seismic Data Processing Methods to Suppress the Acquisition Footprint, SPG/SEG International Geophysical Conference, Expanded Abstracts.

Soubaras, R., 2002, Attenuation of acquisition footprint for non-orthogonal 3D geometries, SEG International Exposition and 72nd Annual Meeting, Expanded Abstracts.

APPENDIX

Software modules used in this study are shown below. All listed functions are Matlab code found in the CREWES Matlab distribution.

ccfoot.m … basic numerical computation of the grid correlations and the numerical grids themselves.

seisplotsvd_sep.m … interactive tool for SVD separation and the estimation of grid correlations.

seisplotsvd_foot … interactive tool for applying wavenumber filters to SVD separations of time slices.